3810 *Chem. Mater.* **2009,** *21,* 3810–3815
DOI:10.1021/cm9009628

CHEMISTRY OF MATERIALS
Article

Reversible Methane Storage in a Polymer-Supported Semi-Clathrate Hydrate at Ambient Temperature and Pressure

Weixing Wang, Benjamin O. Carter, Christopher L. Bray, Alexander Steiner, John Bacsa, James T. A. Jones, Catherine Cropper, Yaroslav Z. Khimyak, Dave J. Adams, and Andrew I. Cooper*

Department of Chemistry, University of Liverpool, Crown Street, Liverpool L69 7ZD, U.K.

Received April 7, 2009. Revised Manuscript Received June 29, 2009

A key issue regarding the use of clathrates and semi-clathrate hydrates for practical gas storage is the pressure−temperature stability of the material. For many practical applications, the avoidance of cooling, gas overpressure, and mechanical mixing would be very desirable. Here, we show that porous emulsion-templated polymer supports greatly enhance methane uptake kinetics in tetra-*iso*-amylammonium bromide semi-clathrate hydrates without introducing complex mixing technologies. These systems show unprecedented thermal stability and can be decomposed upon demand to release the gas. Single crystal X-ray structure analysis of the semi-clathrates loaded with methane or krypton were obtained, confirming that the gases are stored in the dodecahedral A′ and A″ cages.

Introduction

There is much interest currently in the storage of gases such as methane and hydrogen. It is conceptually very appealing to consider systems which will store such gases at ambient pressure and temperature, such that the gas can be transported without any complex containment or cooling and then released (for example, by mild heating) at the point of delivery. Gas hydrates, or gas clathrates, are non-stoichiometric, crystalline inclusion compounds composed of a hydrogen-bonded lattice of water which traps small molecules within polyhedral cavities.[1,2] One volume of methane gas hydrate (MGH) can yield approximately 180 v/v STP methane.[3] It has thus been suggested that it may be economically feasible to transport methane or natural gas in hydrated form. However, bulk hydrate formation rates may be extremely slow, and interstitial water is often trapped in the hydrate.[4,5] Common methods for increasing clathrate formation kinetics include grinding and sieving ice particles to increase the surface area,[6] addition of surfactants,[7] or dispersion of the water phase over silica.[8,9] We recently showed that porous, emulsion-templated polymers can greatly increase the rate of H_2 uptake in THF-stabilized clathrates, but this approach was less successful for MGH.[10] We also showed that "dry water" may be used to dramatically enhance CH_4 uptake rates in MGH.[11] The limited stability of MGH necessitates temperatures near 273 K and a substantial overpressure of CH_4. The "dry water" system adsorbs methane in the absence of mixing, but droplet destabilization over a number of charge−discharge cycles necessitates re-mixing of the dry water for effective re-use.[11] A major practical challenge is to address both stability issues (that is, lower gas storage pressures, higher storage temperatures) as well as the problems of slow kinetics and poor clathrate conversions without compromising the storage capacity of the MGH.

Semi-clathrate hydrates of quaternary ammonium salts such as tetra-*n*-butylammonium bromide (TBAB), tetra-*n*-butylammonium fluoride (TBAF), and tetra-*iso*-amylammonium bromide (TiAAB) are stable to temperatures above 273 K.[12−14] Semi-clathrate hydrates share many of the structural and physical properties of true clathrates. The cation is situated within framework cavities while the anion

*Corresponding author. E-mail: aicooper@liv.ac.uk.

(1) Sloan, E. D.; Koh, C. A. *Clathrate Hydrates of Natural Gases*, 3rd ed.; CRC Press: Boca Raton, 2008.
(2) Koh, C. A. *Chem. Soc. Rev.* **2002**, *31*, 157–167.
(3) Sloan, E. D. *Nature* **2003**, *426*, 353–359.
(4) Englezos, P.; Kalogerakis, N.; Dholabhai, P. D.; Bishnoi, P. R. *Chem. Eng. Sci.* **1987**, *42*, 2647–2658.
(5) Englezos, P.; Kalogerakis, N.; Dholabhai, P. D.; Bishnoi, P. R. *Chem. Eng. Sci.* **1987**, *42*, 2659–2666.
(6) Strobel, T. A.; Taylor, C. J.; Hester, K. C.; Dec, S. F.; Koh, C. A.; Miller, K. T.; Sloan, E. D. *J. Phys. Chem. B* **2006**, *110*, 17121–17125.
(7) Zhang, J. S.; Lee, S.; Lee, J. W. *Ind. Eng. Chem. Res.* **2007**, *46*, 6353–6359.
(8) Anderson, R.; Chapoy, A.; Tohidi, B. *Langmuir* **2007**, *23*, 3440–3444.
(9) Anderson, R.; Llamedo, M.; Tohidi, B.; Burgass, R. W. *J. Phys. Chem. B* **2003**, *107*, 3507–3514.
(10) Su, F.; Bray, C. L.; Tan, B.; Cooper, A. I. *Adv. Mater.* **2008**, *20*, 2663–2666.
(11) Wang, W. X.; Bray, C. L.; Adams, D. J.; Cooper, A. I. J. Am. Chem. Soc. **2008**, *130*, 11608−11609.
(12) Dyadin, Y. A.; Bondaryuk, I. V.; Aladko, L. S. *J. Struct. Chem.* **1995**, *36*, 995–1045.
(13) McMullan, R.; Jeffrey, G. A. *J. Chem. Phys.* **1959**, *31*, 1231–1234.
(14) Aladko, L. S.; Dyadin, Y. A.; Rodionova, T. V.; Terekhova, I. S. *J. Struct. Chem.* **2002**, *43*, 990–994.

Published on Web 08/03/2009

occupies sites in the hydrogen-bonded framework. Semi-clathrate hydrates of TBAB and TBAF have been shown to trap H_2 in the two small, unoccupied lattice cavities.[15,16] These materials are significantly more stable than other H_2 hydrates, with H_2-TBAF hydrates melting at around 302 K.[16] Here, we report the structure, kinetics, and methane storage behavior of a polymer-supported TiAAB semi-clathrate and show that methane gas can be adsorbed quickly in the absence of mixing and released on demand, albeit with relatively low storage capacities of up to 40 v/v.

Experimental Section

Materials. The methane used was UHP 99.999% grade, BOC Gases, Manchester, U.K. All other reagents and solvents were purchased from Sigma-Aldrich or Pfaltz and Bauer (U.K.) and used as received. The polymer support was prepared as before.[10] TiAAB was prepared as described previously.[17]

Characterization. Crystallographic data were recorded on a Bruker Smart Apex diffractometer ($T = 100$ K) using Mo Kα radiation ($\lambda = 0.71073$ Å, $2\theta\max = 55°$). Structures were refined by full-matrix least squares against F^2 using all data.[18] Powder X-ray diffraction data were collected with Cu Kα_1 radiation with a Stoe Stadi-P diffractometer in transmission geometry, using a linear position sensitive detector. Data were collected at room temperature, from $2\theta = 5-40°$, in 0.5° steps at 40 s/step. Samples were prepared by drawing hot (50 °C) solutions of TiAAB·38H_2O and TiAAB·26H_2O into 0.5 mm bore capillaries. Each was sealed at both ends with vacuum grease before allowing the semi-clathrate solution to cool to room temperature. The samples were able to crystallize in situ without risk of phase transition due to loss of coordinating water.

Powder X-ray diffraction patterns were analyzed using Stoe WinXPow v. 1.10 software. Unit cell parameters for the TiAAB·38H_2O crystal structure were used to index and refine both samples. Peaks not observed in the simulated powder pattern for TiAAB·38H_2O were eliminated before indexing and refining all remaining peak positions. The resulting unit cell parameters for both samples indicate an expected thermal expansion, on account of single-crystal XRD data collection taking place at 100 K.

For solid-state NMR analysis, the semi-clathrate TiAAB·38H_2O was taken out of the 68.0 cm^3 high pressure stainless steel cell (New Ways of Analytics, Lörrach, Germany) at ambient temperature and loaded immediately into a 7 mm outer diameter rotor. The rotor was fitted with a BN_3 VT cap containing a hole to prevent any pressure build-up in the event of gas loss. The rotor was then placed into a pre-cooled probe at 273 K, spun at an MAS rate of 3.2 kHz, and cooled further to 263 K. After the initial experiments at 263 and 253 K, the rotor was removed from the probe and placed in a fridge at 278 K overnight prior to experiments at 223 K.

$^1H-^{13}C$ variable temperature (VT) cross-polarization magic angle spinning (CP/MAS) and $^{13}C\{^1H\}$ NMR spectra were recorded using the 7 mm probehead at 263, 253, and 223 K. The spectra were acquired at 400.16 MHz and 100.56 MHz for ^1H and ^{13}C, respectively, at an MAS rate 3.2 kHz. The bearing gas was cooled by passing through a heat exchanger placed in liquid N_2 with the temperature regulation controlled using the standard Bruker heating system. The thermocouple was placed at the bearing gas port inside the probehead stator to obtain the most accurate measurements. In general, the sample was allowed to equilibrate for 30 minutes at each temperature. For the CP experiments, the ^1H $\pi/2$ pulse length was of 6.0 μs and the recycle delay was of 8.0 s. Two phase pulse modulation (TPPM) decoupling was used during acquisition at an rf field of 47.2 kHz. The CP contact time was 4.0 ms with the Hartmann-Hahn matching condition set using hexamethylbenzene (HMB). $^{13}C-\{^1H\}$ VT MAS NMR spectra were recorded using a $\pi/3$ ^{13}C pulse length of 2.9 μs and the recycle delay of 20.0 s. TPPM decoupling at an rf field of 47.2 kHz was used during acquisition.

Clathration Kinetics. Stock solutions of tetra-*iso*-amylammonium bromide with a stoichiometric composition of TiAAB·26H_2O and TiAAB·38H_2O were prepared. To carry out the gas uptake kinetic experiments, 20.0 g of a stock solution of TiAAB was loaded into a 68.0 cm^3 high pressure stainless steel cell (New Ways of Analytics, Lörrach, Germany) together with the polyHIPE support (3.4 g). The temperature was controlled by a programmable thermal circulator (HAAKE Phoenix II P2, Thermo Electron Corporation). The temperature of the compositions in the high pressure cell was measured using a type K thermocouple (Cole-Parmer, −250−400 °C). The gas pressure was monitored using a high-accuracy gauge pressure transmitter (Cole-Parmer, 0−3000 psia). Both thermocouple and transmitter were connected to a digital universal input panel meter (Cole-Parmer), which communicates with a computer. Prior to experiments, the cell was slowly purged with methane three times at atmospheric pressure to remove any air and then pressurized to the desired pressure at the designated temperature. The temperature (T, K), pressure (P, psia), and time (t, min) were automatically interval-logged using MeterView 3.0 software (Cole-Parmer). Using this setup it was possible to obtain high resolution data (for example, 2 s between individual [T, P, t] points, 120 000 data points in a 2000 min experiment). The apparatus is shown schematically elsewhere.[11]

Differential Scanning Calorimetry (DSC). A methane-loaded TiAAB·38H_2O sample (200 mg) was prepared by cooling from 318 K to 273 K under pressure of methane (8.6 MPa). Using a Q2000 DSC instrument, a 10 mg sample was loaded at 273 K using aluminium sample and reference pans. Data were collected at a heating rate of 0.5 K/min from 272 to 318 K. For the methane-loaded samples, the material was melted at 318 K to release methane before allowing semi-clathrate to reform at 273 K. DSC data collection was then carried out as above for the vacant TiAAB·38H_2O sample.

Balloon Release Experiment. A 50 mL round-bottomed flask was loaded with 40 g of TiAAB·26H_2O semi-clathrate hydrate and 6.8 g of polyHIPE. The open flask was pressurized with methane to 9 MPa at 317 K in a 600 cm^3 stainless steel pressure vessel (Parr Instrument Company, U.S.A.). After slowly cooling to 298 K overnight using a water bath, the vessel was vented and the flask fitted with a balloon, before being immersed in iced water for 5 h. After warming to room temperature, little gas was released after standing for 4 h. The flask was then heated to 313 K, at which point all methane was released from the clathrate within 30 min.

Results and discussion

Three stable, gas-free polyhydrates of TiAAB were reported previously.[17] We targeted two compositions: a

(15) Hashimoto, S.; Sugahara, T.; Moritoki, M.; Sato, H.; Ohgaki, K. *Chem. Eng. Sci.* **2008**, *63*, 1092–1097.
(16) Chapoy, A.; Anderson, R.; Tohidi, B. *J. Am. Chem. Soc.* **2007**, *129*, 746–747.
(17) Aladko, L. S.; Dyadin, Y. A.; Mikina, T. V. *Russ. J. Gen. Chem.* **2003**, *73*, 503–506.
(18) Sheldrick, G. M. *Acta Crystallogr., Sect. A* **2008**, *64*, 112–122.

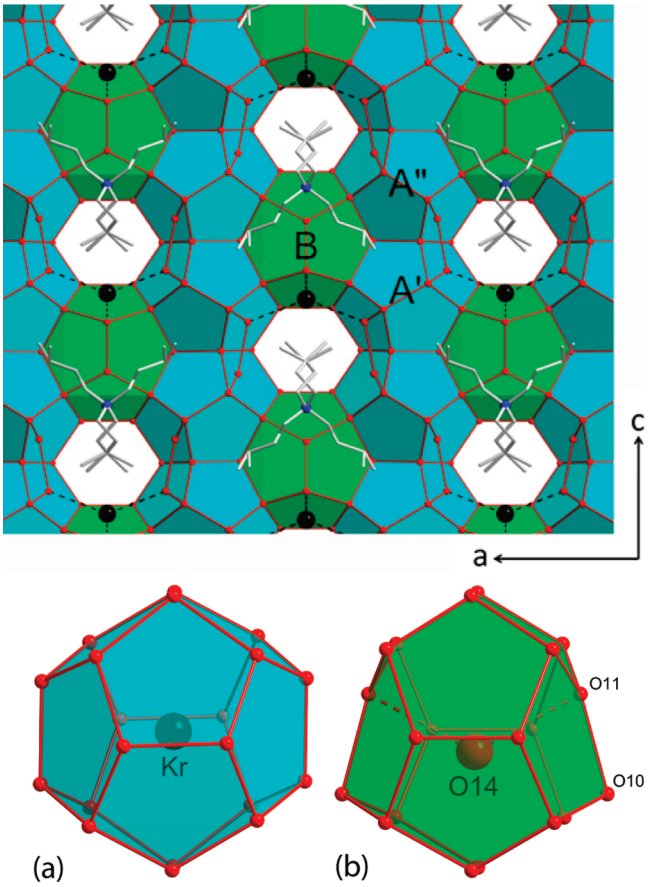

Figure 1. Upper: Crystal structure of the semi-clathrate TiAAB·38H_2O, highlighting the arrangement of dodecahedral cages (A-type, blue; B-type, green). Lower: (a) A-cage hosting CH_4 or Kr, respectively (host-to-O distances: 3.7−4.1 Å); (b) B-cage hosting a water molecule (host-to-O distances: 3.2−4.4 Å), the dashed lines indicate the short distance of 3.2 Å between the host and the trigonal planar nodes of the framework.

3.7 mol % solution (nominal composition TiAAB·26-H_2O) and a 2.6 mol % solution (TiAAB·38H_2O). Single crystals suitable for X-ray structure analysis were obtained for the gas-free semi-clathrate and for CH_4- and krypton-loaded systems. The gas-containing semi-clathrates were grown under gas pressures of 8.6 MPa and found to be sufficiently stable to allow mounting of crystals under ambient (*T*, *P*) conditions. The semi-clathrate framework is *iso*-structural to that of [R_4N]-X·38H_2O (R = *i*Am, X = F[19] and R = R = *n*Bu, X = Br[20]) and crystallizes in the orthorhombic spacegroup *Pmma*. The unit cell contains two 46-hedral cages accommodating the tetraalkyl ammonium ions and six dodecahedral cages that are potential hosts for small molecules.[21] There are two types of dodecahedral cages (labeled A and B in Figure 1): The unique cages A′ and A″ (symmetry 2/*m*) approximate regular dodecahedra and are enclosed exclusively by tetrahedral water molecule nodes. In contrast, cage B (symmetry *mm*2) is distorted as a result of the presence of two nearly planar trigonal framework nodes

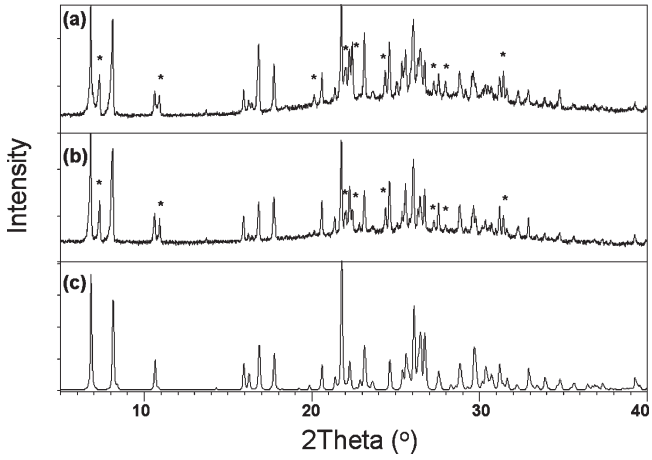

Figure 2. Powder XRD data for (a) TiAAB·38H_2O "feed" composition; (b) TiAAB·26H_2O composition; (c) simulated XRD pattern from single crystal data of TiAAB·38H_2O. Simulated pattern peak positions were corrected to lower 2θ values to take into account the thermal contraction of the unit cell parameters in the single crystal data. Peaks not observed in the simulated powder pattern for TiAAB·38H_2O were eliminated before indexing and refining all remaining peak positions in (a) and (b) and are marked with *.

(O11). These interact only with water molecules of cage B and are denting into the cage (see also Figure S1 in Supporting Information).

The crystal structures show that CH_4 and krypton are accommodated exclusively in cages A. Only the crystals that were grown under pressurized atmospheres of CH_4 and krypton exhibit sharp electron density peaks at the centers of A′ and A″, while no significant electron density was observed in the A-cages of the gas-free crystals. Refinement as C and Kr gave well-defined atom positions with occupancy factors that translate into gas uptakes of 0.6 and 0.9 molar equivalents of CH_4 and krypton, respectively.

The centers of the B-cages of all three compounds exhibit high electron densities. However, these densities do not correlate with the amount of gas-uptake in neighboring A-cages. Certainly, the highly distorted geometry of the B-cage should prohibit the accommodation of Kr or CH_4. The close proximity of the trigonal node O11 to the central peak position (3.2 Å) is well below the sum of the van der Waals radii of O and Kr or methane.[22,23] It has been discussed that these distorted dodecahedra host water molecules, which connect via hydrogen bonds to the somewhat unsaturated trigonal nodes of the framework.[24,25] The refinement of O14, the O-atom of the hosted water molecule, gives long but reasonable O···O distances for hydrogen bonding considering its somewhat diffuse character within the cage. The relatively large thermal parameter indicates that the position of O14 is not as well-defined as that of the hosts accommodated in A-cages. The final occupancy factors of O14 refined to

(19) Feil, D.; Jeffrey, G. A. *J. Chem. Phys.* **1961**, *35*, 1863–1873.
(20) Shimada, W.; Shiro, M.; Kondo, H.; Takeya, S.; Oyama, H.; Ebinuma, T.; Narita, H. *Acta Crystallogr., Sect. C* **2005**, *61*, O65–O66.
(21) Jeffrey, G. A. *J. Incl. Phenom.* **1984**, *1*, 211–222.
(22) Kobayashi, R.; Katz, D. L. *Trans. Am. Inst. Mining Metall. Eng.* **1949**, *186*, 66–70.
(23) Bondi, A. *J. Phys. Chem.* **1964**, *68*, 441–451.
(24) Bonamico, M.; McMullan, R. K.; Jeffrey, G. A. *J. Chem. Phys.* **1962**, *37*, 2219−2231.
(25) Komarov, V. Y.; Rodionova, T. V.; Terekhova, I. S.; Kuratieva, N. V. *J. Incl. Phenom. Macrocyclic Chem.* **2007**, *59*, 11–15.

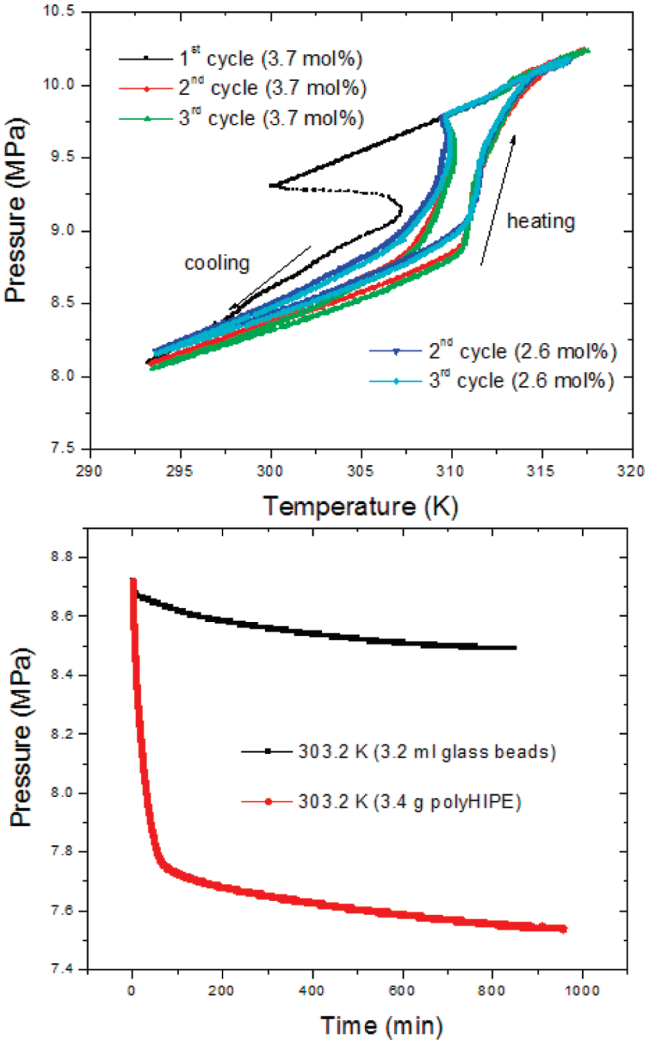

Figure 3. Upper: $P-T$ plot for polymer-supported TiAAB·26H_2O (black/red/green curves) and TiAAB·38H_2O (blue curves) (20 g solution, 3.4 g polymer support), cooling/heating rate = 2 K/h. Lower: Kinetic plots for CH_4 encapsulation in TiAAB−H_2O semi-clathrate hydrate supported on polymer at 303 K (20 g TiAAB·26H_2O, 3.4 g polyHIPE with "bulk" control experiment using glass beads as volumetric filler (equivalent to volume of the polymer).

0.23(2) for the gas-free derivative, 0.18(2) for the crystals loaded with methane, and 0.48(2) for the crystals charged with krypton. This variation may result from the kinetics of the clathration in different experiments, which are known to be stochastic.[1] Figure 1 (lower) shows the dodecahedral cages A and B together with their guests. Taking the hosted water molecules into account, the overall sum formulas of the three structurally determined systems are [iAm$_4$N]Br·38.2H_2O, [iAm$_4$N]Br·38.2H_2O·0.62CH_4, and [iAm$_4$N]Br·38.5H_2O·0.91Kr, respectively.

Powder X-ray diffraction (PXRD) data demonstrate that TiAAB·38H_2O is formed preferentially over TiAAB·26H_2O irrespective of the prepared water content in the salt solution (Figure 2). Comparison with the simulated PXRD pattern generated from single-crystal XRD data shows good agreement with the data obtained for both samples. In both cases, extra peaks are apparent (* in Figure 2a,b), possibly indicative of a different crystal

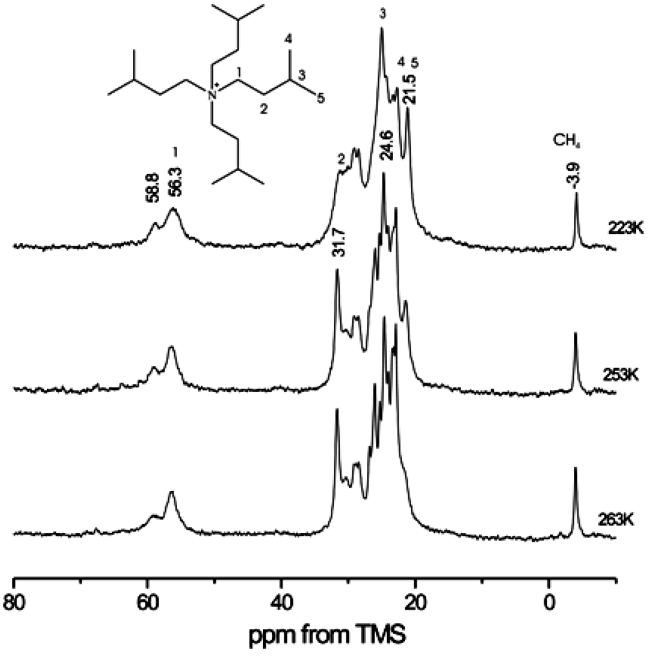

Figure 4. $^{13}C\{^1H\}$ MAS NMR spectra of H_2O−TiAAB−CH_4 semi-clathrate recorded at various temperatures.

form. Theoretical PXRD peak positions generated from TBAB·26H_2O crystal parameters[26] include a diffraction peak at $2\theta = 7.39°$, in agreement with the additional experimental peak at this 2θ observable in Figure 2. We therefore ascribe the extra peaks to being consistent with TiAAB·26H_2O hydrate coexisting with the 38H_2O material. This is difficult to corroborate in the absence of relative peak intensities or complete crystal data for either TBAB·26H_2O or TiAAB·26H_2O, although we note that Lipkowski et al. reported kinetic difficulties in preparing the analogous tetra-*iso*-amylammonium fluoride (TiAAF·27H_2O), with TiAAF·38H_2O being formed in preference.[27] The data in Figure 2 confirm that the dominant species in both cases is TiAAB·38H_2O. Indexing the PXRD spectra gave cell parameters for the TiAAB·38H_2O feed composition of a = 21.669(6) Å, b = 12.932(3) Å, and c = 12.026(3) Å with a cell volume = 3369.9(11) Å^3 and for the TiAAB·26H_2O feed composition of a = 21.683(10) Å, b = 12.928(5) Å, and c = 12.026(5) Å and a cell volume = 3371.0(18) Å^3. These values are slightly larger than those found from the single crystal data above (see ESI), which is to be expected considering the higher temperature at which the PXRD data were collected.

We next investigated the storage of methane within a TiAAB semi-clathrate supported on an ultralow-density, emulsion-templated "polyHIPE" material.[10] The interconnected pore structure and very low bulk density allowed us to support 20 g of TiAAB solution on 3.4 g of the polymer. Figure 3 shows a $P-T$ plot for the CH_4−TiAAB−H_2O system. With no support, the $P-T$ relationship

(26) Gaponenko, L. A.; Solodovnikov, S. F.; Dyadin, Y. A.; Aladko, L. S.; Polyanskaya, T. M. *J. Struct. Chem.* **1984**, *25*, 157–159.
(27) Lipkowski, J.; Suwinska, K.; Rodionova, T. V.; Udachin, K. A.; Dyadin, Y. A. *J. Incl. Phenom. Mol. Recognit. Chem.* **1994**, *17*, 137–148.

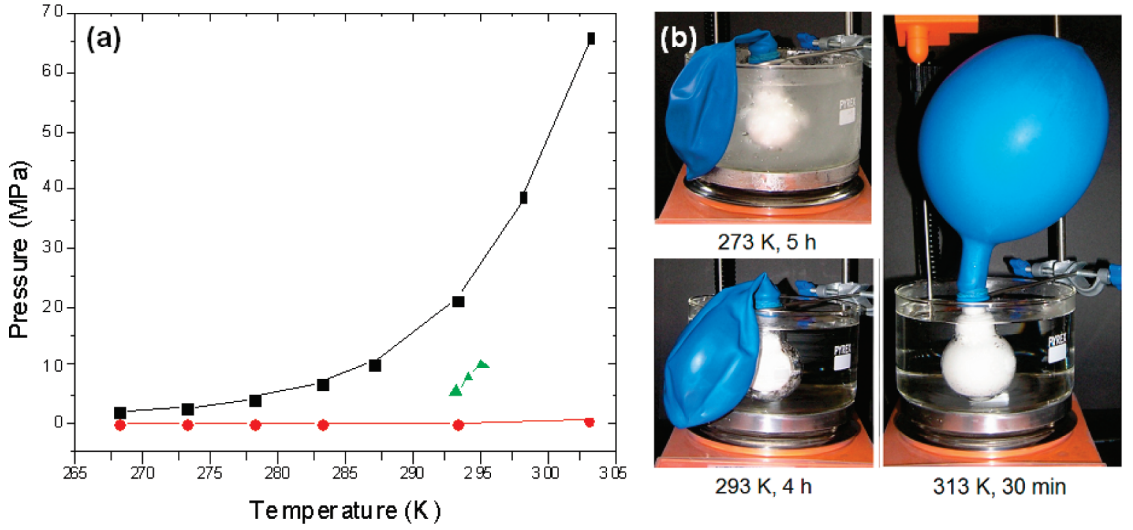

Figure 5. (a) Stability of $CH_4-TiAAB-H_2O$ clathrate hydrate (20g 3.7 mol % TiAAB solution supported on 3.4 g polymer, red) as compared to sI MGH (data calculated using CSMPlug,[1] black) and $CH_4-TBAB-H_2O$ clathrate hydrate[15] (green). (b) Photographs showing $CH_4-TiAAB-H_2O$ stability at 273 K and 1 bar (5 h; left top), and 293 K and 1 bar (4 h; left bottom) and CH_4 dissociation and release at 313 K (right).

for CH_4 in the system approximated to the ideal gas law during the heating/cooling cycle (data not shown); that is, very little CH_4 clathrate was formed in the bulk in the absence of mixing. By contrast, clathrate formation and subsequent dissociation occurred in the presence of the polymer support, as evidenced by the significant pressure drop on cooling and the pressure rise on heating (Figure 3, upper). On repeating this cycle, the clathration onset temperature increased substantially (310 K versus 300 K in the first cycle). Further repeats of the heating/cooling cycle (up to 20 repeats) then closely follow the second cycle. We speculate that this first "induction cycle" may result from the more uniform distribution of the TiAAB/water system throughout the hydrophobic polymer support, as discussed previously for polymer-supported $THF-H_2O-H_2$ clathrates.[10] However, it may also arise from the clathrate memory effect that has been reported for a number of different systems.[1] Data for the 2.6 mol % solution closely followed that for the 3.7 mol % solution, again supporting the preferential formation of $TiAAB \cdot 38H_2O$.

The kinetics of clathration and gas uptake capacity were both greatly enhanced by the presence of the polymer support (Figure 3, lower). Again, this effect is reproducible over multiple charge−discharge cycles. The CH_4 capacity derived from the pressure drop, ΔP (1.18 MPa), at 303.2 K was estimated to be 36.8 v/v relative to the amount of $TiAAB-H_2O$ added, as calculated using GasPak v3.41 software. Volumetric release experiments confirmed this capacity. This equates to approximately 80% of the maximum theoretical capacity as calculated for the system based on complete filling of both available small A cages (Figure 1). The time to reach 90% saturation capacity, t_{90}, was ~200 min whereas very little CH_4 uptake was observed in the bulk unmixed system on this time scale (Figure 3, lower).

The CH_4 encapsulation capacity was also confirmed by ^{13}C MAS NMR. The $^1H-^{13}C$ CP/MAS NMR spectra of the supported semi-clathrate all show peaks corresponding to the aromatic protons in the polyHIPE support (127.6 ppm). The peaks at 40.8 and 29.0 ppm correspond to the aliphatic resonances of the emulsion-templated polymer support (see Figure S4, Supporting Information). Both $^1H-^{13}C$ CP/MAS (see Figure S2, Supporting Information) and $^{13}C\{^1H\}$ MAS NMR (Figure 4) spectra show several resonances attributable to TiAAB. A number of peaks are observed for the terminal methyl and methyne sites. This is due to the interactions of the salt with the clathrate framework and their restricted mobility. The assignment of the resonances due to the template has been confirmed using the $^1H-^{13}C$ dipolar dephasing experiments (see Figure S3, Supporting Information). Peaks at approximately 57 ppm correspond to $-N-CH_2-$ sites. Peaks at approximately 32 ppm correspond to $N-CH_2-CH_2-$. The two populations for the $-N-CH_2-$ sites indicate the presence of two motionally different environments for the salt. The peak at 56.3 ppm is observed in both the $^1H-^{13}C$ CP/MAS and $^{13}C\{^1H\}$ MAS NMR spectra (Figures 4 and S2, Supporting Information). The resonance at 58.8 ppm has been observed using $^1H-^{13}C$ CP/MAS experiments only at 223 K, while being present in the $^{13}C\{^1H\}$ MAS NMR spectra at all temperatures studied. Most probably the latter environment is due to a disordered salt species with enhanced mobility, hence not registering in the CP spectra at 253 and 263 K.

The ratio between the intensities of the $N-CH_2$ peak at 56.3 ppm and methane guest peak at −3.7 ppm (spectra measured at 263 K) was determined to be approximately 2.7: this suggests 81% of the maximum available uptake capacity (as determined from the crystal structure). The ratio between the $N-CH_2$ resonance at 56.3 ppm and that of methane at 223 K after storage in the fridge overnight (278 K) was found to be approximately 4.2 (56% of the maximum loading). The slightly lower CH_4 occupancy (62%) compared to that estimated from single crystal X-ray could be explained by sample morphology (much

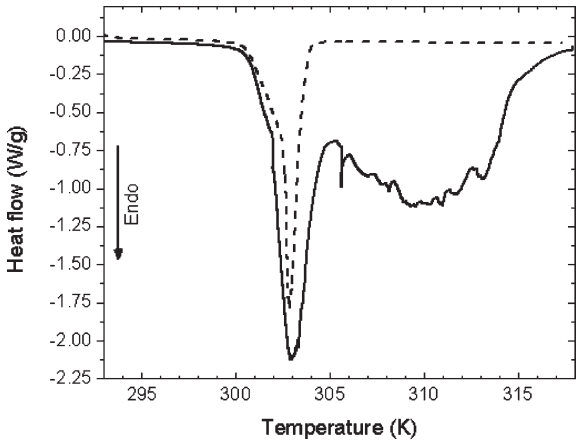

Figure 6. Differential scanning calorimetry for TiAAB−H_2O clathrate hydrate (dashed line) and CH_4−TiAAB−H_2O clathrate (solid line).

smaller polymer-supported domains versus much larger single crystals in X-ray experiments).

A key issue regarding the use of clathrate and semi-clathrate hydrates for practical gas storage is the pressure−temperature stability of the material. For many practical applications, the avoidance of cooling, gas overpressure, and mechanical mixing would be very desirable. The stability of the CH_4−TiAAB−H_2O semi-clathrate hydrate was found to be much higher than the sI MGH (Figure 5a).

To further examine the thermal stability of the CH_4−TiAAB−H_2O clathrate, we used differential scanning calorimetry (DSC) to determine the enthalpies of melting for the TiAAB clathrate hydrate and for the same material containing methane (Figure 6). The neat TiAAB clathrate hydrate melted at approximately 303 K. The CH_4−TiAAB−H_2O also demonstrated a melting point at 303 K, followed by a broad transition centered around 310 K (Figure 6). These transitions correlate well with the expected melting point of TiAAB clathrate hydrate[28] and also correlate with the temperatures recorded for clathration onset and decomposition at high pressures (Figure 3). Similar observations have been made in other studies which did not involve TiAAB;[29,30] in those cases, a melting transition for the ice framework was observed followed by a second transition as the methane clathrate melts.[29] These data further illustrate the thermal stability of the CH_4−TiAAB−H_2O hydrate.

We also compared the CH_4−TiAAB−H_2O with the CH_4−TBAB−H_2O system,[31,32] used previously to store both CH_4 and H_2. TiAAB CH_4 semi-clathrate hydrate exhibits enhanced stability over the TBAB system. The *iso*-amyl chains fill the available cavity more effectively than butyl chains and hence exert a greater stabilizing effect on the H_2O cages.[14] Indeed, this system retained clathrated CH_4 after several hours at room temperature. Figure 5b demonstrates that no CH_4 is evolved after 5 h at 273 K, as indicated by the deflated balloon. On warming to 293 K, virtually no gas is evolved after a further 4 h. Upon warming to 303 K, the clathrated gas is evolved rapidly, inflating the balloon. This behavior is in total contrast to CH_4 storage in porous physisorptive materials.[33−35] We estimate that the H_2O−TiAAB−CH_4 system is around 8 K more stable than comparable TBAB systems,[32] a relatively small difference but important in terms of pushing stabilities above "ambient" temperature. The absence of stirring is also significant: previous studies with TBAB[32] involved vigorous mechanical mixing under pressure using an impeller. Reversible storage (Figures 3 and 5) using a static, lightweight polymer support with no moving parts may be a much more practical solution for many applications.

Conclusions

In summary, we have shown that emulsion-templated polymer supports greatly enhance CH_4 uptake kinetics in semi-clathrate hydrates without introducing complex mixing technologies. These systems show unprecedented thermal stability and can be decomposed upon demand to release the gas. The system is reversible with no degradation in performance over at least 20 charge/discharge cycles. This combines for the first time a number of important practical considerations in a single gas storage system. We also demonstrate unambiguously that CH_4 and Kr are stored in the dodecahedral cages A′ and A″ which have 2/*m* symmetry. The main practical drawback of the system is the relatively low CH_4 capacity with respect to pure MGH (35−40 v/v versus 180 v/v). Indeed, this may be insurmountable in the present system since the enhanced stability of the semi-clathrate hydrate arises from the substantial cage filling that occurs. We are currently investigating approaches to combine these promising stability and recyclability advantages with less compromised gas storage capacities, for example, by designing salts which exert equivalent stabilization effects while filling fewer cages. This system also provides a possible "blueprint" for other systems: for example, wholly organic gas clathrates or hydrogel systems[36] dispersed on high pore-volume organic polymer supports.

Acknowledgment. We acknowledge EPSRC (EP/511794/1, EP/G006091/1, EP/F06229X/1) for funding this research. A.I. C. is a Royal Society Wolfson Research Merit Award holder.

Supporting Information Available: Further crystallographic details and solid state NMR of the TiAAB semi-clathrates (PDF). This material is available free of charge via the Internet at http://pubs.acs.org.

(28) Aladko, L.S.; Dyadin, Y. A.; Rodionova, T. V.; Terekhova, I. S. *J. Mol. Liquids* **2003**, *106*, 229–238.
(29) Giavarini, C.; Maccioni, F.; Santareli, M. L. *J. Therm. Anal. Calorim.* **2006**, *84*, 419–424.
(30) Giavarini, C.; Maccioni, F.; Politi, M.; Santareli, M. L. *Energy Fuels* **2007**, *21*, 3284–3291.
(31) Li, D. L.; Du, J. W.; Fan, S. S.; Liang, D. Q.; Li, X. S.; Huang, N. S. *J. Chem. Eng. Data* **2007**, *52*, 1916–1918.
(32) Arjmandi, M.; Chapoy, A.; Tohidi, B. *J. Chem. Eng. Data* **2007**, *52*, 2153–2158.
(33) Wood, C. D.; Tan, B.; Trewin, A.; Su, F.; Rosseinsky, M. J.; Bradshaw, D.; Sun, Y.; Zhou, L.; Cooper, A. I. *Adv. Mater.* **2008**, *20*, 1916–1921.
(34) Rowsell, J. L. C.; Spencer, E. C.; Eckert, J.; Howard, J. A. K.; Yaghi, O. M. *Science* **2005**, *309*, 1350–1354.
(35) Ma, S. Q.; Sun, D. F.; Simmons, J. M.; Collier, C. D.; Yuan, D. Q.; Zhou, H. C. *J. Am. Chem. Soc.* **2008**, *130*, 1012–1016.
(36) Su, F.; Bray, C. L.; Carter, B. O.; Overend, G.; Cropper, C.; Iggo, J. A.; Khimyak, Y. Z.; Fogg, A. M.; Cooper, A. I. *Adv. Mater.* **2009**, *21*, 2383–2386.